

## Eye-specific visual processing in the mouse suprachiasmatic nuclei

Lauren Walmsley & Timothy M Brown\*

Faculty of Life Sciences, University of Manchester, UK

\*AV Hill Building

University of Manchester

Oxford Road

Manchester

M13 9PT

[timothy.brown@manchester.ac.uk](mailto:timothy.brown@manchester.ac.uk)

- Daily changes in global levels of illumination synchronise daily physiological rhythms via bilateral retinal projections to the suprachiasmatic nuclei.
- We aimed to determine how retinal signals are integrated within the suprachiasmatic nuclei.
- By monitoring electrophysiological responses to visual stimuli we show that most suprachiasmatic neurons receive input from just one eye.
- Our results establish that suprachiasmatic neurons measure local light intensity and that any assessment of global light levels occurs at the network level.

### Abstract

Internal circadian clocks are important regulators of mammalian biology, acting to coordinate physiology and behaviour in line with daily changes in the environment. At present, synchronisation of the circadian system to the solar cycle is believed to rely on a quantitative assessment of total ambient illumination, provided by a bilateral projection from the retina to the suprachiasmatic nuclei (SCN). It is currently unclear, however, whether this photic integration occurs at the level of individual cells or within the SCN network. Here we use extracellular multielectrode recordings from the SCN of anaesthetised mice to show that most SCN neurons receive visual input from just one eye. While we find that binocular inputs to a subset of cells are important for rapid responses to changes in illumination, we find no evidence indicating that individual SCN cells are capable of reporting the average light intensity across the whole visual field. As a result of these local irradiance coding properties, our data establish that photic integration is primarily mediated at the level of the SCN network and suggest that accurate assessments of global light levels would be impaired by non-uniform illumination of either eye.

**Abbreviations** ipRGC, intrinsically photosensitive retinal ganglion cell; SCN, suprachiasmatic nuclei

## Introduction

The ability to anticipate recurring changes in the environment is crucial to the survival of all organisms. One especially pervasive mechanism by which this is achieved is via internal circadian clocks which can be synchronised to daily variations in the environment, most notably the solar cycle (Roenneberg *et al.*, 1997). In mammals this process thus relies on direct retinal projections to the hypothalamic suprachiasmatic nuclei (SCN), site of the master circadian pacemaker (Golombek *et al.*, 2010; Lucas *et al.*, 2012).

It has long been recognised that the quality of visual information that would be useful to the SCN is quite distinct from that which is important for more conventional visual pathways. Thus, retinal pathways supplying the thalamocortical visual system are organised to allow for a relatively stable representation of form and motion across the  $\sim 9$  decimal orders of light intensity that separate the darkest night and the brightest day (Rieke *et al.*, 2009). By contrast, detailed information about spatiotemporal patterns of illumination is presumably unimportant to the circadian system, which instead requires an accurate readout of global light intensity to infer time-of-day.

Consistent with this view, numerous behavioural studies have demonstrated that the response of the circadian system to light can be accurately predicted based on the total number of photons that the animal is exposed to (Dkhissi-Benyahya *et al.*, 2000; Lall *et al.*, 2010; Lucas *et al.*, 2012; Nelson *et al.*, 1999; Nelson *et al.*, 1991). Thus, for example, short bright light pulses evoke a similar adjustment in clock phase as longer dimmer stimuli. Although there are known specific situations where this relationship breaks down (Lall *et al.*, 2010; Vidal *et al.*, 2007), the accepted model of clock resetting is one whereby the retinorecipient SCN act as a photon counter and controls circadian responses accordingly.

The intuitive separation between the desired properties of conventional and circadian visual processing is also supported by extensive anatomical data. Hence, retinal projections to conventional visual targets in the thalamus/tectum arise primary via the contralateral hemisphere, with ipsilateral projections coming exclusively from regions of the retina corresponding to the zone of binocular overlap (Coleman *et al.*, 2009; Morin *et al.*, 2014; Sterratt *et al.*, 2013). By contrast, the SCN receives dense bilateral retinal innervation (Morin *et al.*, 2014). Moreover, it is now clear that this retinal input to the SCN derives primarily from a subclass of intrinsically photosensitive retinal ganglion cell (ipRGC), termed M1 (Hattar *et al.*, 2006). These cells appear specialised to encode irradiance and, unusually, projected bilaterally to the brain (Brown *et al.*, 2010; Brown *et al.*, 2011; Hattar *et al.*, 2006)- even

where their retinal location places their field of view far outside the region of binocular overlap (Muscat *et al.*, 2003).

This anatomical arrangement seems ideally placed to allow individual SCN neurons to measure the average light intensity from across the full visual field although, to date, this hypothesis remains untested. Existing data suggest that removing signals from one eye produces larger than expected deficits in circadian phase shifting and/or SCN Fos induction (Muscat *et al.*, 2005; Tang *et al.*, 2002). However, none of the many studies investigating visual response properties within the SCN (Aggelopoulos *et al.*, 2000; Brown *et al.*, 2011; Drouyer *et al.*, 2007; Meijer *et al.*, 1986; Meijer *et al.*, 1992; Mure *et al.*, 2007; Nakamura *et al.*, 2004; Sakai, 2014; van Diepen *et al.*, 2013) have extensively characterised binocular processing at the level of individual neurons. Here we set out to address this issue, via multielectrode recordings from mouse SCN neurons using visual stimuli designed to determine the nature and extent of ipsi-/contralateral visual signals, both across the population and on individual cells.

## **Methods**

### *Animals*

All animal use was in accordance with the Animals, Scientific Procedures, Act of 1986 (UK). Experiments were performed on adult male (50-80 days) *Opn4*<sup>+/tau-lacZ</sup> reporter mice and wildtype (*Opn4*<sup>+/+</sup>) littermates (n=19 & n=14 respectively). Consistent with previous reports (Hattar *et al.*, 2003; Howarth *et al.*, 2014; Lucas *et al.*, 2003), there were no observable abnormalities in the visual responses of reporter animals, hence the two datasets were combined for the analysis presented in this study. Prior to experiments, animals were housed under a strict 12-hour dark/light cycle environment at a temperature of 22°C with food and water ad libitum.

### *In Vivo Neurophysiology*

In preparation for stereotaxic surgery, mice were removed from their housing environment ~2-3h before lights off and anaesthetised with urethane (1.55g/kg i.p in 0.9% sterile saline). Mice were then prepared for stereotaxic surgery as previously described (Brown *et al.*, 2011). Recording probes (Buszaki 32L; Neuronexus, MI, USA) consisting of 4 shanks (spaced 200µm), each with 8 closely spaced recordings sites in diamond formation (intersite distance 20-34µm) were coated with fluorescent dye (CM-Dil; Invitrogen, Paisley, UK) and then inserted into the brain parallel to the midline, 1mm lateral and 0.3mm caudal to bregma (centre of probe) at an angle of 9° relative to the dorsal-ventral axis. Electrodes were then

lowered to the level of the SCN using a fluid filled micromanipulator (MO-10, Narishige International Ltd., London, UK).

After allowing 30min for neural activity to stabilise following probe insertion, wideband neural signals were acquired using a Recorder64 system (Plexon, TX, USA), amplified (x3000) and digitized at 40kHz. Action potentials were discriminated from these signals offline as 'virtual'-tetrode waveforms using custom MATLAB (The Mathworks Inc., MA, USA) scripts and sorted manually using commercial principle components based software (Offline sorter, Plexon, TX, USA) as described previously (Howarth *et al.*, 2014). All surgical procedures were completed before the end of the home cage light phase, such that electrophysiological recordings spanned the late projected day-mid projected night, an epoch when the SCN light response is most sensitive (Brown *et al.*, 2011).

### *Visual Stimuli*

Light measurements were performed using a calibrated spectroradiometer (Bentham instruments, Reading, UK).

Full field visual stimuli were generated via two LEDs ( $\lambda_{max}$  410nm; half-width:  $\pm 7$ nm; Thorlabs, NJ, USA) independently controlled via LabVIEW (National Instruments, TX, USA) and neutral density filter wheels (Thorlabs). Light was supplied to the subject via 7mm diameter flexible fibre optic light guides (Edmund Optics; York, UK), positioned 5mm from each eye and enclosed within internally reflective plastic cones that fit snugly over each eye to prevent off-target effects due to scattered light. Responses to these stimuli were then assessed as follows:

To determine the relative magnitude and sensitivity of eye specific responses in SCN neurons, mice were maintained in darkness and 5s light steps were applied in an interleaved fashion to contra- and/or ipsilateral eyes for a total of 10 repeats at logarithmically increasing intensities spanning 9.8-15.8 log photons/cm<sup>2</sup>/s (interstimulus interval 20-50s depending on intensity). Because all mouse photoreceptors display similar sensitivity to the wavelengths contained in our stimuli (Brown *et al.*, 2013; Brown *et al.*, 2012), after correction for pre-receptor filtering (Govardovskii *et al.*, 2000; Jacobs *et al.*, 2007), effective photon fluxes for each mouse opsin were between 0.5 (M- and S-cone opsins) and 0.3 log units (melanopsin) dimmer than this value. Intensities reported in the manuscript reflect effective irradiance for rod opsin, which is intermediate between these extremes (9.4-15.4 log photons/cm<sup>2</sup>/s).

To determine components of the SCN response that were dependent on stimulus brightness vs. stimulus contrast, a second protocol was also employed. Here we stepped light intensity independently at each eye every 5s in a pseudorandom sequence spanning effective irradiances between 10.4-15.4 log photons/cm<sup>2</sup>/s (total number of steps =840). The sequence was generated such that, at any one time, the difference in intensity between the two eyes was no more than 2 decimal units and the instantaneous step in light intensity at each eye was one of five possible values ( $\pm 2$ , 1 or 0 log units). To determine contrast-dependent components we then averaged cellular responses (0-500ms post change in light intensity) as a function of step magnitude at either eye. Since we found that contrast response relationships varied very little as a function of absolute irradiance data reported in the manuscript were averaged across all irradiances tested. For clarity, we only present data for steps providing contrast at one eye or equal contrast at both eyes.

To assess SCN response components that tracked stimulus brightness, we reanalysed the above to extract steady state firing (1s epochs occurring at least 4s after step in light intensity) as a function of absolute irradiance at either eye (independently or in combination).

### *Histology*

At the end of each experiment, mice were perfused transcardially with 0.1M phosphate buffered saline followed by 4% paraformaldehyde. The brain was removed, post-fixed in 4% paraformaldehyde for 30min and subsequently cryoprotected in 30% sucrose. The following day, brains were sectioned (100-150 $\mu$ m) on a freezing sledge microtome and either mounted directly onto slides (wildtype mice) using Vectasheild (Vectorlaboratories Ltd., Peterborough, UK) or first processed for X-gal staining (Opn4<sup>+/*tau-lacZ*</sup>) as described below.

X-gal staining was performed as previously described (Hattar *et al.*, 2006). Brain sections were washed twice for 10 minutes each in buffer B (0.1M PBS at pH 7.4, 2mM MgCl<sub>2</sub>, 0.01% Na-desoxycholate and 0.02% IGEPAL). Sections were then incubated for 4 hours in staining solution [buffer B with potassium ferricyanide (5mM), potassium ferrocyanide (5mM) and X-gal (Bioline Reagents Ltd, UK; 1mg/ml)] at 37°C in darkness. Following staining, sections were washed twice for 5 minutes in 0.1M PBS and mounted to slides using Vectashield as above.

After mounting Dil-labelled probe placements were visualised under a fluorescent microscope (Olympus BX51) with appropriate filter sets and, where appropriate, X-gal staining was visualised by standard light microscopy (Fig 1A). Resulting images were then compared with appropriate stereotaxic atlas figures (Paxinos, 2001), using the optic chiasm,

SCN and 3<sup>rd</sup> ventricle as landmarks, to confirm appropriate probe placement. Consistent with previous anatomical and neurophysiological studies (Brown *et al.*, 2011; Hattar *et al.*, 2006; Morin *et al.*, 2014; Nakamura *et al.*, 2004), visually evoked activity was exclusively observed at electrode sites located within the SCN or its immediate borders (Fig. 1).

### *Data analysis*

In most cases, single cell responses are presented as the mean $\pm$ SEM change in firing across all trials (at least 10 per stimulus) relative to baseline (average firing rate 3 or 5s before step in light intensity for light- and dark-adapted responses respectively). Measures of monocular preference were calculated as  $(\text{Response}_{\text{CONTRA}} - \text{Response}_{\text{IPSI}}) / (\text{Response}_{\text{CONTRA}} + \text{Response}_{\text{IPSI}})$ , such that contralateral biased responses tended towards 1 and ipsilateral biased responses towards -1. Where a cell did not show a significant response to stimulation of one of the two eyes (paired t-test between firing during first 500ms of light step and baseline,  $P > 0.05$ ), that response component was assigned a value of zero. The eye that evoked the largest response when analysed in this way was designated the 'dominant' eye. Binocular facilitation was analysed in a similar way:  $(\text{Response}_{\text{BOTH}} - \text{Response}_{\text{DOMINANT}}) / (\text{Response}_{\text{BOTH}} + \text{Response}_{\text{DOMINANT}})$ . We classified as binocular any cell exhibiting significant responses to stimulation of both eyes individually or where the response to binocular stimulation was significantly different to that evoked by stimulating the dominant eye alone (unpaired t-test based on response to 10 trials of each stimulus).

Where average population data is presented, in most cases responses were baseline subtracted (as above) and normalised on a within cell basis according to the largest response within a specific protocol. The exception to this rule was our analysis of brightness coding, where the absolute firing rates of each cell were normalised to range between zero and one before averaging across the population.

Statistical analyses were performed using GraphPad Prism v.6 (Graphpad Software Inc., CA, USA). Data were, in most cases, fit by 4-parameter sigmoid curves with the minimum constrained to zero as appropriate. Comparisons of sensitivity under various conditions were assessed by F-test for differences in  $EC_{50}$ , hill slope and/or maxima. Influences of eye-specific brightness/contrast on responses of various cell types were analysed by 2-way repeated measures ANOVA with dominant and non-dominant eye stimuli as factors.

## **Results**

### ***Binocular influences on SCN population activity***

We first set out to determine how binocular signals were integrated to influence population firing activity within the SCN. To this end we performed multielectrode (32 channel) extracellular recordings of multiunit activity from the SCN and surrounding hypothalamus (n=33 mice) and monitored responses to full field stimuli (410nm LED; 5s from darkness), applied at varying intensity to one or both eyes. Since all mouse photoreceptor classes are equally sensitive in this part of the spectrum (see Methods), any heterogeneity in the photoreceptor populations driving specific responses (Brown *et al.*, 2011; van Oosterhout *et al.*, 2012) should not influence sensitivity as assessed under these conditions.

Surprisingly, given the reported dense bilateral retinal innervation of the mouse SCN (Brown *et al.*, 2010; Hattar *et al.*, 2006; Morin *et al.*, 2014), we found that responses driven by the contralateral retina were reliably larger than those resulting from stimulation of the ipsilateral eye (Fig. 2A,B; n=252 electrodes exhibiting visually evoked activity). Thus although the sensitivity of ipsi/contralateral responses were similar (F-test for difference in EC<sub>50</sub> and/or Hill slope; P=0.64) the maximum amplitude of these were ~2-fold greater following stimulation of the contralateral eye (F-test for difference in saturation point, P=0.003). Interestingly, responses evoked by stimulating both eyes together were especially large. In line with the above, this significant difference in maximal response (F-test vs. contralateral only; P<0.001) was not associated with any appreciable difference the sensitivity of binocular vs. monocular responses (P=0.77).

Importantly, we found that SCN population activity driven by stimulation of both eyes was statistically indistinguishable from a simple linear sum of the observed responses to stimulating either eye alone (Fig. 2B; F-test, P=0.69). This surprising result indicates that SCN population activity does not accurately follow the total number of photons detected across both retinae. If this were the case then, correcting for the 2-fold difference in total light intensity, the average response across the paired SCN to monocular stimuli should be identical to that of an equivalent irradiance stimulus applied to both eyes. In fact, we found that the monocular responses were markedly smaller than expected given the binocular photon-response relationship (Fig. 2C; F-test, P<0.001). Indeed, to evoke a 50% maximal change in SCN population activity, monocular stimuli would need to be ~100 fold brighter than would be sufficient for light detected at both eyes.

### ***Binocular integration in individual SCN neurons.***

Our data above reveal that population activity within the SCN does not (at least in all cases) exhibit the strict photon counting properties one might predict based on previous behavioural experiments (Dkhissi-Benyahya *et al.*, 2000; Lall *et al.*, 2010; Lucas *et al.*, 2012; Nelson *et*

*al.*, 1999; Nelson *et al.*, 1991). Given this unexpected result, we next aimed to determine how these tissue level visual response properties arise through the sensory characteristics of individual SCN neurons.

From our multiunit recordings we were able to isolate the activity of 61 individual cells within or bordering the SCN, of which 51 were light sensitive. Across this population, we observed heterogeneity in eye specific responses to light steps from darkness (Fig. 3A-E). This included many cells that responded solely to stimulation of either the contralateral (Fig. 3A,E; n=15) or ipsilateral eye (Fig. 3B,E; n=19) and other cells that exhibited clear responses to stimulation of either eye and/or substantially larger responses to binocular vs. monocular stimulation (Fig. 3C-E; n=17).

Thus, we found that the majority (~67%) of visually responsive SCN neurons did not integrate binocular signals and, instead, faithfully reported monocular irradiance (Figure 3F). In all cases, responses of these cells to stimulation of the dominant eye vs. both eyes were statistically identical (Fig. 3E; t-tests based on responses to 10 trials,  $P > 0.05$ ).

By contrast, for the smaller proportion of SCN cells that did have access to visual signals from either eye, responses were in most cases biased towards one retina, with the binocular influence most evident as an enhanced response to stimulation of both eyes (Fig. 3E,G). Surprisingly, here we found that average binocular responses were in fact significantly larger than even a linear sum of the two monocular inputs (F-test for difference in saturation point,  $P = 0.007$ ; not shown). This synergistic effect appeared to diminish over time, however (Fig. 3C,D), such that towards the end of the light steps (last 1s) responses were not significantly different from the linear prediction (F-test,  $P = 0.69$ ).

Together, these SCN cellular properties explain the unexpectedly small SCN multiunit responses to monocular vs. binocular stimuli (Fig. 2) – most SCN neurons are strongly biased towards one eye such that at any given intensity many more cells will be activated by stimulating both eyes. Surprisingly, however, the observed multiunit bias towards contralateral driven visual responses (Fig. 2B) did not translate into an increased number of contralateral biased SCN neurons. In fact, we observed statistically equivalent proportions of ipsi-/contralateral biased SCN neurons (n=27 and 24 respectively, Fishers exact test,  $P = 0.77$ ). These data imply that, across the population, contralateral inputs tend to drive larger responses in individual SCN neurons than do ipsilateral inputs (although among the sample of cells we collected this difference did not attain significance:  $3.8 \pm 0.7$  vs.  $2.7 \pm 0.7$  spikes/s respectively at  $15.4 \log$  photons/cm<sup>2</sup>/s; paired t-test,  $P = 0.28$ ).



In sum, our data above suggest that while a subset of SCN neurons receives inputs from both eyes, none of these cells alone can effectively integrate photons from across the visual scene to report the total amount of light in the environment. It is worth noting, however, that such light steps applied from darkness represent rather unnatural visual stimuli. Moreover, these do not allow one to distinguish response components that are dependent on the absolute irradiance of the signal vs the relative change in irradiance (brightness vs. contrast). To better understand, then, how SCN neurons track spatio-temporal variations in light intensity under more natural conditions we next assessed responses to smaller modulations in light intensity, using a protocol that allowed us to dissociate response components dependent on stimulus brightness vs. contrast.

#### *Response properties of SCN binocular cells*

Since our data indicated that binocular influences were especially pronounced for the initial components of SCN neuronal responses under dark adapted conditions, we first examined how binocular cells responded to acute changes in light intensity in the range up to  $\pm 2$  log units, applied under light adapted conditions (11.4 to 14.4 log photons/cm<sup>2</sup>/s).

Interestingly, we found that when changes in light intensity occurred simultaneously across both eyes, binocular cells exhibited very sharp and robust increases or decreases in firing (Fig. 4A) that were near-linear with respect to the log change in irradiance (Fig. 4B). By contrast, responses were smaller and much more sluggish when light steps occurred solely at the dominant eye and were virtually undetectable when applied to the non-dominant eye (Fig. 4A,B). Together, these data indicate that binocular integration functions in this population of cells to facilitate rapid responses to global changes in light levels.

We next determined the extent to which eye-specific signals influenced the ability of binocular cells to track brightness (Fig. 5A), by quantifying steady state firing (4-5s after a change in light intensity) as a function of absolute irradiance. Given the data described above, one might expect the steady state firing of binocular cells to be strongly influenced by the overall irradiance across either eye. In fact, however, we found very little influence of binocular integration on the steady state firing of such cells. Thus, rather than following the mean irradiance across both eyes (Fig. 5B, F-test,  $P < 0.001$ ) binocular cell firing activity was, instead, entirely accounted for by the irradiance at the dominant eye, regardless of the interocular difference in brightness (Fig. 5C, F-test,  $P = 0.62$ ). Intriguingly, then, despite clear binocular influences on responses to rapid changes in light levels, basal firing of binocular cells was entirely driven by just one of the two eyes.

### *Response properties of SCN monocular cells*

To better understand how the properties of binocular cells, outlined above, distinguished them from other visually responsive (monocular) SCN neurons, we also examined brightness and contrast components of the monocular cell responses.

Surprisingly, we found that whereas binocular cells reliably exhibited 'ON' responses to visual contrast (i.e. a positive relationship between the step in light intensity and change in firing), only a subset of monocular cells exhibited this property (Fig. 6A;  $n=24/34$ ). Other cells exhibited decreases in firing in response to increased light intensity (OFF,  $n=5$ ) or displayed transient increases in firing in response to both light increments and decrements (ON/OFF,  $n=5$ ).

Unlike binocular cells (Fig. 6B), all these monocular populations exhibited robust, near-log linear, changes in firing as a function of step magnitude at the dominant eye alone (Fig. 6B). Moreover, none of these monocular populations displayed any clear influence of non-dominant eye contrast, (2-way repeated measures ANOVA, non-dominant eye and interaction terms all  $P>0.05$ ).

We have previously reported 'transient' cells in the mouse SCN (Brown *et al.*, 2011), whose visual response properties appear consistent with those of the ON/OFF cells described above. By contrast, the presence of monocular cells exhibiting OFF responses under these conditions was surprising – not least because all of these cells exhibited excitatory responses to light steps applied from darkness (not shown). Interestingly, these OFF responses also appeared to exclusively originate with the ipsilateral eye (Fig. 6B). Based on our sample size there is a low probability that we could have failed to detect an equivalent population of contralateral-driven OFF cells (Fishers exact test,  $P=0.053$ ). In sum then it appears that ipsilateral retinal influences on the SCN may be more diverse than the primarily ON responses originating with the contralateral eye (Fig. 6B).

In line with their responses to visual contrast described above, we found that, whereas the steady state firing of ON cells reliably increased as a function of monocular brightness, that of OFF cells decreased (Fig. 7A,B). Importantly, we were also able to identify both ON and OFF cells within the same recording (Fig. 7A), indicating that this unusual OFF behaviour could not simply reflect some state or circadian phase-dependent switch in general SCN responsiveness.

By contrast with the other SCN cell types, the steady state activity of ON/OFF cells did not vary as a function of irradiance (Fig. 8, repeated measures ANOVA,  $P=0.36$ ), indicating that this population specifically responds only to rapid changes in light intensity.

## Discussion

Here we show that, despite the dense bilateral input that the SCN receive from the retina (Brown *et al.*, 2010; Hattar *et al.*, 2006; Miura *et al.*, 1997; Morin *et al.*, 2014), few individual SCN neurons have access to visual signals from both eyes. Moreover, even where cells do receive input from both eyes, binocular influences are limited to just the initial components of any response to changing irradiance. As a result, no single SCN neuron is capable of providing direct information about global levels of irradiance across the full visual field.

These results are surprising for two reasons. Firstly because we have previously observed extensive binocular integration in the mouse visual thalamus, a region where eye-specific inputs were, until recently, believed to remain entirely segregated (Howarth *et al.*, 2014). Indeed, using similar approaches to those employed here, we observed many single cells in the visual thalamus whose basal firing did encode mean binocular irradiance. More importantly, however, our present results are unexpected because the existing model posits that circadian photoentrainment is reliant on a quantitative assessment of the total amount of light in the environment (Dkhissi-Benyahya *et al.*, 2000; Lall *et al.*, 2010; Lucas *et al.*, 2012; Nelson *et al.*, 1999; Nelson *et al.*, 1991). Assuming this model correct, any such assessment of global irradiance could occur neither at the level of individual cells, nor by simply taking the average light-evoked activity across the population of such cells.

In fact, since the degree of visually evoked SCN activity is well correlated with the magnitude of circadian phase shifts (Brown *et al.*, 2011; Meijer *et al.*, 1992), our present data suggest that the current model of circadian photic integration is not entirely accurate. Based on the light-evoked firing we observe in the SCN, we would predict that light falling on one, rather than both, eyes would result in a 50% reduction in phase shift magnitude, rather than a 50% reduction in apparent light intensity (0.3 log units). As far as we are aware, only one study has explicitly tested this possibility, by performing a reversible monocular occlusion before applying phase shifting light stimuli (Muscat *et al.*, 2005). Unfortunately, inter-individual variability in phase shift magnitude make a robust assessment of the above difficult although, for long/bright stimuli, monocular phase shifts certainly appear better explained by a 50% reduction in amplitude rather than in total photon flux.

Accordingly, we propose that retinorecipient SCN neurons do accurately measure photon flux, but only within a portion of the visual field. Based on an established view of SCN organisation, suggesting the presence of weak oscillators that are readily reset by light and robust oscillators which integrate circadian inputs from the former (Albus *et al.*, 2005; Brown *et al.*, 2009; Rohling *et al.*, 2011), we propose a model whereby the retinorecipient cells are reset according to 'local' light intensity (Fig. 9). It is then the average phase information supplied by these retinorecipient oscillators that dictates the integrated circadian response. Such a mechanism would account for the behavioural response to monocular visual stimuli and the associated 50% reduction in the number of Fos-positive SCN neurons previously observed (Muscat *et al.*, 2005).

We should also note that another study, employing unilateral optic nerve transection, found a much larger (~90%) reduction in light-induced Fos across the hamster SCN (Tang *et al.*, 2002). The reason for this discrepancy is unclear but, again, this observation appears hard to incorporate into a model whereby the SCN response is proportional to the total level of ambient illumination.

Aside from the above, there have been very few investigations of cellular level integration of binocular signals in the SCN. Thus, most previous investigations of neurophysiological effects of light in the SCN have used exclusively monocular (Brown *et al.*, 2011; Meijer *et al.*, 1986; Nakamura *et al.*, 2004) or binocular stimuli (Aggelopoulos *et al.*, 2000; Drouyer *et al.*, 2007; Meijer *et al.*, 1992; Mure *et al.*, 2007; van Diepen *et al.*, 2013). A few studies have investigated ocularity of rat, degus and diurnal ground squirrel SCN cells (Jiao *et al.*, 1999; Meijer *et al.*, 1989), but in each case the number of cells (n=3) and irradiance range tested was too low to draw any solid inferences on binocular processing in the clock of these species.

At present, there is also little information about the specific location(s) or number of retinal ganglion cells (RGCs) from which each retinorecipient SCN cell receives input. Whereas RGC projections to more conventional visual centres adopt a specific organisation to facilitate image forming vision (Sterratt *et al.*, 2013), it feels unlikely that something similar should also be true for the SCN. Indeed, the SCN is known to deviate from this scheme by virtue of the fact it receives input from the nasal and superior regions of the ipsilateral retina (Morin *et al.*, 2003). Moreover, while eye-specific inputs to the hamster SCN appear partially anatomically segregated (Muscat *et al.*, 2003) this doesn't seem to hold true the mouse (Brown *et al.*, 2010; Morin *et al.*, 2014). If instead, then, retinal input to SCN neurons is essentially random, our data suggest that the number of RGC inputs to any one cell must be

small. In fact, the near equal numbers of contralateral, ipsilateral and binocularly responsive SCN neurons we observe suggests that, on average, each of these cells samples from 2 RGCs.

If correct, our suggestion above would imply that most SCN neurons could only measure light intensity within very restricted patches of the visual field (<30° given the known dendritic field sizes of the melanopsin RGCs that provide most of the input; (Berson *et al.*, 2010). Accordingly, individual SCN cells could detect quite different daily patterns of illumination (e.g. if they monitored light intensity exclusively from the lower rather than upper visual field). We tentatively suggest that such a mechanism could contribute to the pronounced, photoperiod-dependent, phase differences in the electrical activity exhibited by SCN neurons (Brown *et al.*, 2009; VanderLeest *et al.*, 2007).

It is also interesting to speculate as to the functional significance of the binocular input to a subset of SCN cells. It is clear from our data that this input makes little contribution to irradiance coding and instead acts to promote rapid and robust responses to sudden changes in light intensity. It is currently unclear why such a property would be useful to the clock, however, existing data indicate that high frequency retinal input and subsequent SCN cell firing are important for triggering internal calcium mobilisation (Irwin *et al.*, 2007). It may then be the case that the initial transient response of SCN cells (which often overshoot the steady state level attained for a given irradiance) are especially significant for initiating the intracellular signalling cascade required for phase shifting.

As a final note here, since our SCN recordings were performed in anaesthetised mice, it is important to consider the possibility that responses recorded under our experimental conditions do not fully recapitulate those observed in freely behaving animals. On the basis of the available data, we think it unlikely that the anaesthetic we employ here would result in any qualitative change in the visual responses of SCN neurons. Hence, multiunit recordings in freely moving mice (van Diepen *et al.*, 2013; van Oosterhout *et al.*, 2012) reveal visual responses with essentially identical sensitivity and temporal profile to those we report here and have observed previously (Brown *et al.*, 2011).

Aside from the above, our data also add to existing literature indicating a surprising amount of diversity in the visual responses of hypothalamic neurons (Aggelopoulos *et al.*, 2000; Brown *et al.*, 2011; Drouyer *et al.*, 2007). In line with earlier anatomical data (Guler *et al.*, 2008; Sollars *et al.*, 2003), we previously reported that a subset of cells within or bordering the SCN lacked functional melanopsin input and sustained responses to light (Brown *et al.*,

2011). Another study, performed in awake (head-fixed) mice also reports a small subset of SCN cells with apparently similar properties (Sakai, 2014). Here we confirm that these non-irradiance coding SCN cells in fact specifically encode rapid light increments or decrements. None of these cells exhibited binocular responses, suggesting that this population primarily (if not exclusively) signals visual contrast within a restricted portion of the visual field, as described above for irradiance coding SCN cells. Given these properties, we think it unlikely that such cells play a major role in circadian entrainment, although it is possible that they contribute to more direct SCN-dependent modulations in physiology such as effects on corticosterone secretion (Kiessling *et al.*, 2014).

We also identify an especially unusual population of cells that exhibit OFF responses to visual contrast and whose steady state firing activity is thus inversely related to irradiance. While light-suppressed SCN cells have been reported previously (Aggelopoulos *et al.*, 2000; Brown *et al.*, 2011; Drouyer *et al.*, 2007; Meijer *et al.*, 1986; Meijer *et al.*, 1992), the population of mouse neurons we report here are distinct in that under dark-adapted conditions they display robust excitatory responses. Moreover the inhibitory responses of these OFF cells under light- adaptation are much more rapid than those of the very rare light-suppressed SCN cells we previously reported in the mouse (Brown *et al.*, 2011).

As far as we are aware, then, the ON to OFF switching behaviour we describe above has never previously been reported. Although possible that these observations reflect a circadian phase-dependent effect (light-adapted recordings always followed dark-adapted in our experiments) we think this is unlikely to reflect a global change across the SCN. Hence we routinely observed the more conventional ON responses among simultaneously recorded neurons. It is noteworthy here that all of the OFF cells we recorded were exclusively driven by the ipsilateral retina, suggesting that there may be some differential processing of eye specific signals within the SCN. For example, the switch from excitatory to inhibitory responses might reflect a changing balance between direct and indirect ipsilateral visual input following light adaption. Such indirect visual input could arise locally, via the opposing SCN or indeed via other brain regions such as the intergeniculate leaflet (Blasiak *et al.*, 2013; Howarth *et al.*, 2014; Tang *et al.*, 2002). At present, we can only speculate as to the functional significance of the 'darkness-coding' behaviour that these OFF cells exhibit. Presumably the presence of such cells increase the variety of output signals that the SCN is able to transmit, allowing for differential regulation of various aspects of physiology (Kalsbeek *et al.*, 2006).

In summary, our data provide new insight into the mechanisms through which the circadian clock processes visual signals. Most notably, we show that the ability of individual SCN neurons to detect irradiance is restricted to only a portion of the full visual field. The implication of this arrangement is that asymmetries in the amount of illumination between left and right eyes could lead the circadian system to substantially underestimate the total amount of ambient illumination. Our data thus predict that, in the absence of any compensatory reorganisation, loss of one eye should result in an unexpectedly large deficit in photic integration within the SCN.

## References

### Author Contributions

T.M.B designed the research, L.W. performed the experiments, L.W. & T.M.B. analysed the data, L.W. & T.M.B wrote the manuscript. All experiments were performed at the University of Manchester.

### Funding

This research was supported by a Biotechnology and Biological Sciences Research Council (BBSRC, UK) David Philips fellowship to T.M.B. (BB/I017836/1).

## References

Aggelopoulos NC, Meissl H (2000). Responses of neurones of the rat suprachiasmatic nucleus to retinal illumination under photopic and scotopic conditions. *J Physiol* 523 Pt 1, 211-222.

Albus H, Vansteensel MJ, Michel S, Block GD, Meijer JH (2005). A GABAergic mechanism is necessary for coupling dissociable ventral and dorsal regional oscillators within the circadian clock. *Curr Biol* 15, 886-893.

Berson DM, Castrucci AM, Provencio I (2010). Morphology and mosaics of melanopsin-expressing retinal ganglion cell types in mice. *J Comp Neurol* 518, 2405-2422.

Blasiak T, Lewandowski MH (2013). Differential firing pattern and response to lighting conditions of rat intergeniculate leaflet neurons projecting to suprachiasmatic nucleus or contralateral intergeniculate leaflet. *Neuroscience* 228, 315-324.

Brown TM, Allen AE, al-Enezi J, Wynne J, Schlangen L, Hommes V, Lucas RJ (2013). The melanopic sensitivity function accounts for melanopsin-driven responses in mice under diverse lighting conditions. *PLoS One* 8, e53583.

Brown TM, Gias C, Hatori M, Keding SR, Semo M, Coffey PJ, Gigg J, Piggins HD, Panda S, Lucas RJ (2010). Melanopsin contributions to irradiance coding in the thalamo-cortical visual system. *PLoS Biol* 8, e1000558.

Brown TM, Piggins HD (2009). Spatiotemporal heterogeneity in the electrical activity of suprachiasmatic nuclei neurons and their response to photoperiod. *J Biol Rhythms* 24, 44-54.

Brown TM, Tsujimura S, Allen AE, Wynne J, Bedford R, Vickery G, Vugler A, Lucas RJ (2012). Melanopsin-based brightness discrimination in mice and humans. *Curr Biol* 22, 1134-1141.

Brown TM, Wynne J, Piggins HD, Lucas RJ (2011). Multiple hypothalamic cell populations encoding distinct visual information. *J Physiol* 589, 1173-1194.

Coleman JE, Law K, Bear MF (2009). Anatomical origins of ocular dominance in mouse primary visual cortex. *Neuroscience* 161, 561-571.

Dkhissi-Benyahya O, Sicard B, Cooper HM (2000). Effects of irradiance and stimulus duration on early gene expression (Fos) in the suprachiasmatic nucleus: temporal summation and reciprocity. *J Neurosci* 20, 7790-7797.

Drouyer E, Rieux C, Hut RA, Cooper HM (2007). Responses of suprachiasmatic nucleus neurons to light and dark adaptation: relative contributions of melanopsin and rod-cone inputs. *J Neurosci* 27, 9623-9631.

Golombek DA, Rosenstein RE (2010). Physiology of circadian entrainment. *Physiol Rev* 90, 1063-1102.

Govardovskii VI, Fyhrquist N, Reuter T, Kuzmin DG, Donner K (2000). In search of the visual pigment template. *Vis Neurosci* 17, 509-528.

Guler AD, Ecker JL, Lall GS, Haq S, Altimus CM, Liao HW, Barnard AR, Cahill H, Badea TC, Zhao H, Hankins MW, Berson DM, Lucas RJ, Yau KW, Hattar S (2008). Melanopsin cells are the principal conduits for rod-cone input to non-image-forming vision. *Nature* 453, 102-105.

Hattar S, Kumar M, Park A, Tong P, Tung J, Yau KW, Berson DM (2006). Central projections of melanopsin-expressing retinal ganglion cells in the mouse. *J Comp Neurol* 497, 326-349.

Hattar S, Lucas RJ, Mrosovsky N, Thompson S, Douglas RH, Hankins MW, Lem J, Biel M, Hofmann F, Foster RG, Yau KW (2003). Melanopsin and rod-cone photoreceptive systems account for all major accessory visual functions in mice. *Nature* 424, 76-81.



Howarth M, Walmsley L, Brown TM (2014). Binocular integration in the mouse lateral geniculate nuclei. *Curr Biol* 24, 1241-1247.

Irwin RP, Allen CN (2007). Calcium response to retinohypothalamic tract synaptic transmission in suprachiasmatic nucleus neurons. *J Neurosci* 27, 11748-11757.

Jacobs GH, Williams GA (2007). Contributions of the mouse UV photopigment to the ERG and to vision. *Doc Ophthalmol* 115, 137-144.

Jiao YY, Lee TM, Rusak B (1999). Photic responses of suprachiasmatic area neurons in diurnal degus (*Octodon degus*) and nocturnal rats (*Rattus norvegicus*). *Brain Res* 817, 93-103.

Kalsbeek A, Perreau-Lenz S, Buijs RM (2006). A network of (autonomic) clock outputs. *Chronobiol Int* 23, 521-535.

Kiessling S, Sollars PJ, Pickard GE (2014). Light stimulates the mouse adrenal through a retinohypothalamic pathway independent of an effect on the clock in the suprachiasmatic nucleus. *PLoS One* 9, e92959.

Lall GS, Revell VL, Momiji H, Al Enezi J, Altimus CM, Guler AD, Aguilar C, Cameron MA, Allender S, Hankins MW, Lucas RJ (2010). Distinct contributions of rod, cone, and melanopsin photoreceptors to encoding irradiance. *Neuron* 66, 417-428.

Lucas RJ, Hattar S, Takao M, Berson DM, Foster RG, Yau KW (2003). Diminished pupillary light reflex at high irradiances in melanopsin-knockout mice. *Science* 299, 245-247.

Lucas RJ, Lall GS, Allen AE, Brown TM (2012). How rod, cone, and melanopsin photoreceptors come together to enlighten the mammalian circadian clock. *Prog Brain Res* 199, 1-18.

Meijer JH, Groos GA, Rusak B (1986). Luminance coding in a circadian pacemaker: the suprachiasmatic nucleus of the rat and the hamster. *Brain Res* 382, 109-118.

Meijer JH, Rusak B, Ganshirt G (1992). The relation between light-induced discharge in the suprachiasmatic nucleus and phase shifts of hamster circadian rhythms. *Brain Res* 598, 257-263.

Meijer JH, Rusak B, Harrington ME (1989). Photically responsive neurons in the hypothalamus of a diurnal ground squirrel. *Brain Res* 501, 315-323.

Miura M, Dong K, Ahmed FA, Okamura H, Yamadori T (1997). The termination of optic nerve fibers in the albino mouse. *Kobe J Med Sci* 43, 99-108.

Morin LP, Blanchard JH, Provencio I (2003). Retinal ganglion cell projections to the hamster suprachiasmatic nucleus, intergeniculate leaflet, and visual midbrain: bifurcation and melanopsin immunoreactivity. *J Comp Neurol* 465, 401-416.

Morin LP, Studholme KM (2014). Retinofugal projections in the mouse. *J Comp Neurol* 522, 3733-3753.

Mure LS, Rieux C, Hattar S, Cooper HM (2007). Melanopsin-dependent nonvisual responses: evidence for photopigment bistability in vivo. *J Biol Rhythms* 22, 411-424.

Muscat L, Huberman AD, Jordan CL, Morin LP (2003). Crossed and uncrossed retinal projections to the hamster circadian system. *J Comp Neurol* 466, 513-524.

Muscat L, Morin LP (2005). Binocular contributions to the responsiveness and integrative capacity of the circadian rhythm system to light. *J Biol Rhythms* 20, 513-525.

Nakamura TJ, Fujimura K, Ebihara S, Shinohara K (2004). Light response of the neuronal firing activity in the suprachiasmatic nucleus of mice. *Neurosci Lett* 371, 244-248.

Nelson DE, Takahashi JS (1999). Integration and saturation within the circadian photic entrainment pathway of hamsters. *Am J Physiol* 277, R1351-1361.

Nelson DE, Takahashi JS (1991). Sensitivity and integration in a visual pathway for circadian entrainment in the hamster (*Mesocricetus auratus*). *J Physiol* 439, 115-145.

Paxinos GF, K.B.J. (2001). *The mouse brain in stereotaxic coordinates: Second Edition*. edn. Academic Press: San Diego.

Rieke F, Rudd ME (2009). The challenges natural images pose for visual adaptation. *Neuron* 64, 605-616.

Roenneberg T, Foster RG (1997). Twilight times: light and the circadian system. *Photochem Photobiol* 66, 549-561.

Rohling JH, vanderLeest HT, Michel S, Vansteensel MJ, Meijer JH (2011). Phase resetting of the mammalian circadian clock relies on a rapid shift of a small population of pacemaker neurons. *PLoS One* 6, e25437.

Sakai K (2014). Single unit activity of the suprachiasmatic nucleus and surrounding neurons during the wake-sleep cycle in mice. *Neuroscience* 260, 249-264.

Sollars PJ, Smeraski CA, Kaufman JD, Ogilvie MD, Provencio I, Pickard GE (2003). Melanopsin and non-melanopsin expressing retinal ganglion cells innervate the hypothalamic suprachiasmatic nucleus. *Vis Neurosci* 20, 601-610.

Sterratt DC, Lyngholm D, Willshaw DJ, Thompson ID (2013). Standard anatomical and visual space for the mouse retina: computational reconstruction and transformation of flattened retinæ with the Retistruct package. *PLoS Comput Biol* 9, e1002921.

Tang IH, Murakami DM, Fuller CA (2002). Unilateral optic nerve transection alters light response of suprachiasmatic nucleus and intergeniculate leaflet. *Am J Physiol Regul Integr Comp Physiol* 282, R569-577.

van Diepen HC, Ramkisoensing A, Peirson SN, Foster RG, Meijer JH (2013). Irradiance encoding in the suprachiasmatic nuclei by rod and cone photoreceptors. *FASEB J* 27, 4204-4212.

van Oosterhout F, Fisher SP, van Diepen HC, Watson TS, Houben T, VanderLeest HT, Thompson S, Peirson SN, Foster RG, Meijer JH (2012). Ultraviolet light provides a major input to non-image-forming light detection in mice. *Curr Biol* 22, 1397-1402.

VanderLeest HT, Houben T, Michel S, Deboer T, Albus H, Vansteensel MJ, Block GD, Meijer JH (2007). Seasonal encoding by the circadian pacemaker of the SCN. *Curr Biol* 17, 468-473.

Vidal L, Morin LP (2007). Absence of normal photic integration in the circadian visual system: response to millisecond light flashes. *J Neurosci* 27, 3375-3382.

## Figure Legends

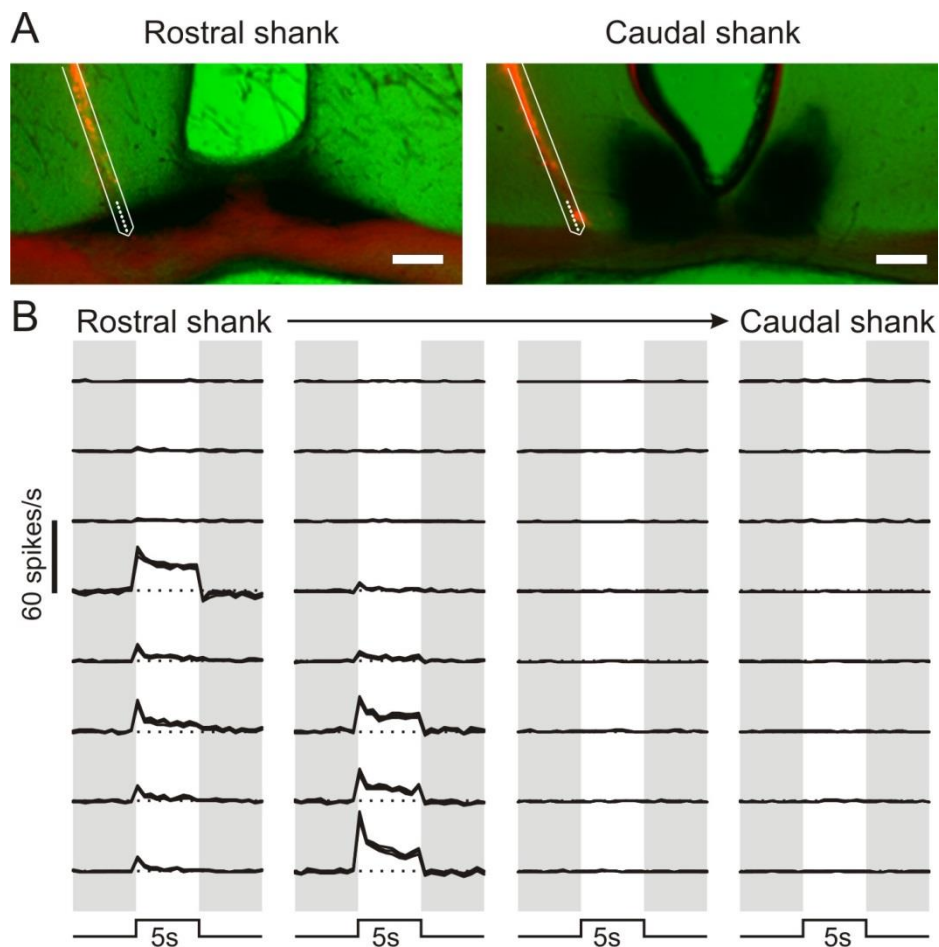


**Figure 1. Light evoked activity in the retinorecipient SCN region. (A)** X-gal stained histological images showing multielectrode placement in the SCN region of an *Opn4<sup>+/tau-lacZ</sup>* reporter mouse. DiI-labelled probe tracks are in red, light microscopy for X-gal staining is pseudocoloured green (with melanopsin ganglion cell projections evident as darkly stained areas). Overlaid schematic (in white) shows projected locations of the 8 recording sites on each shank. Only the most rostral and caudal shanks for the 4-shank electrode are shown. Scale bars=100 $\mu$ m. **(B)** Multiunit activity detected across the 4x8 channel electrode placement shown in **A**, in response to 5s light pulses presented to both eyes (405nm; 15.4 log photons/cm<sup>2</sup>/s). Traces represent the mean $\pm$ SEM change in firing (from 10 trials) over baseline (represented by dotted lines). Note that visual responses are absent from electrode sites located outside of the retinorecipient SCN region such as upper sites on the rostral shank and all sites on the caudal shank.

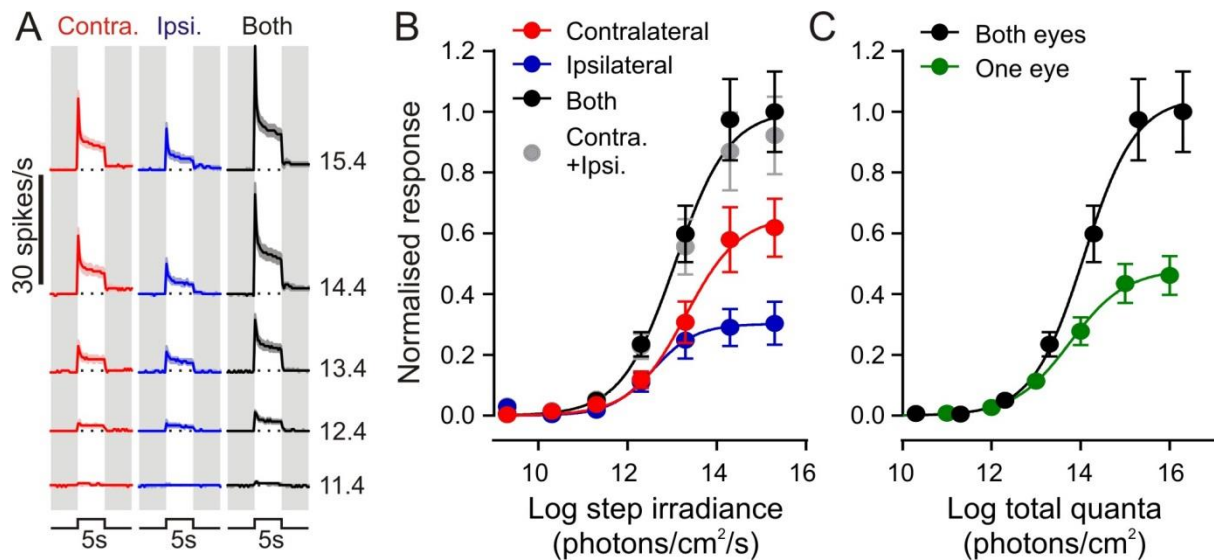


**Figure 2. SCN population firing activity does not faithfully report global irradiance. (A)** Mean  $\pm$  SEM multiunit firing response profile across the retinorecipient SCN-region (n=252 electrodes from 33 mice) in response to 5s light steps (410nm LED, effective intensities 11.4-15.4 log photons/cm<sup>2</sup>/s, from darkness) targeting the contralateral and/or ipsilateral eye. Data were normalised by subtracting pre-stimulus (5s before light on) firing rates (represented by dotted lines). **(B)** Normalised multiunit firing response (change in spike rate averaged across 5s light on, mean  $\pm$  SEM) as a function of step irradiance. Responses to stimulating both eyes together were statistically indistinguishable from a linear sum of the measured response evoked by stimulation of contralateral and ipsilateral eyes alone (grey symbols, F-test, P=0.69). **(C)** Normalised multiunit firing response (conventions as in **B**), plotted as a function of total number of photons delivered. The predicted average across left and right SCN (green symbols; average of ipsilateral and contralateral responses from **B**) is significantly lower than the response to stimulating both eyes even when corrected for total number of photons (F-test, P<0.0001).

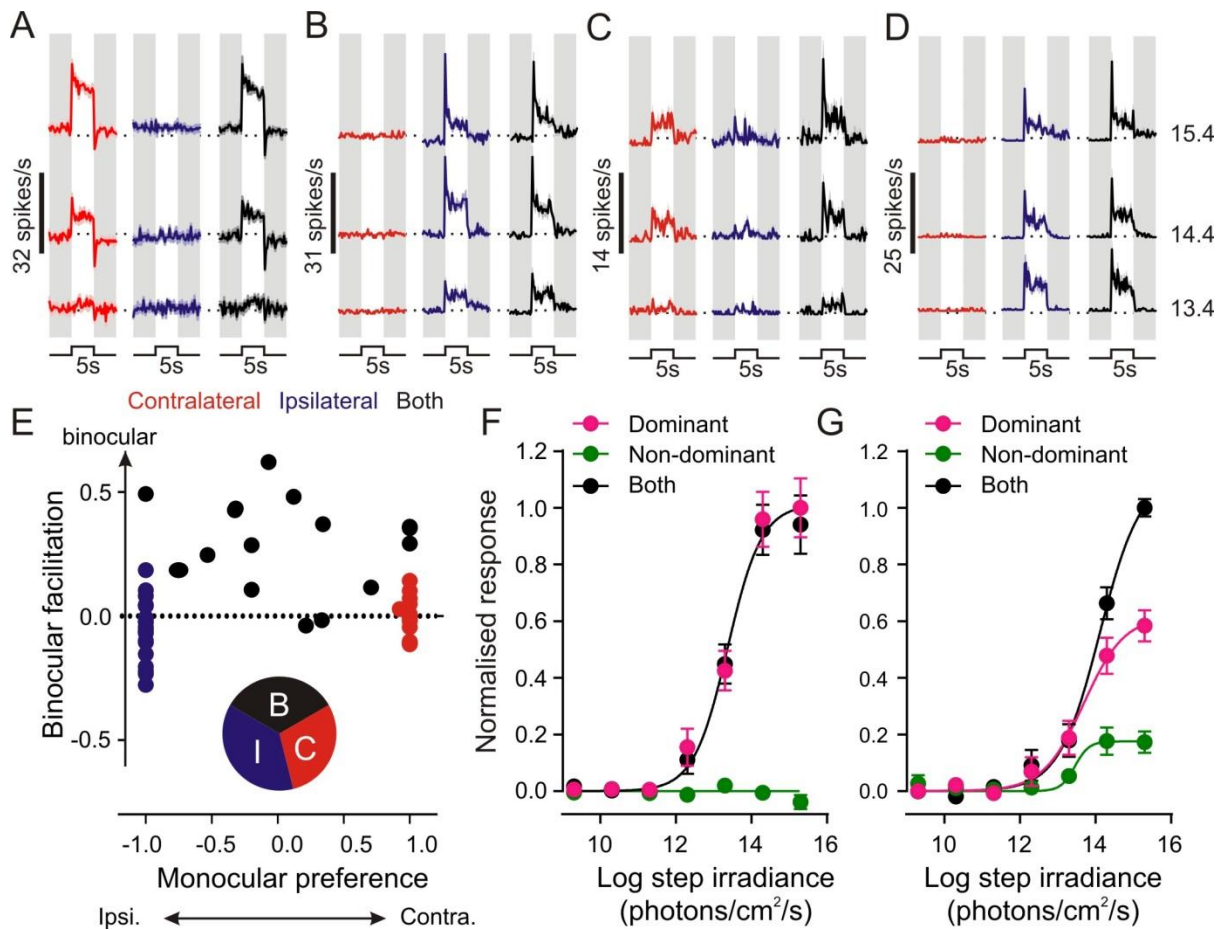


**Figure 3. Eye-specific response properties of SCN neurons.** (A-D) Example firing response profiles (mean±SEM of 10 trials) for 4 SCN single units in response to 5s light steps (410nm LED, effective intensities 13.4-15.4 log photons/cm<sup>2</sup>/s, from darkness) targeting the contralateral and/or ipsilateral eye. Many cells only showed clear responses to stimulation of either contralateral (A) or ipsilateral (B) eye, while a subset showed binocular responses or varying strength (C,D). (E) Population data for 51 visually response SCN neurons showing monocular preference (0=equally matched binocular response) vs. binocular facilitation (positive values= larger response to stimulation of both eyes vs. one eye; see methods for details). Inset pie chart shows proportion of cells exhibiting purely ipsilateral, contralateral or binocular responses. (F) Normalised acute response of monocular cells (change in spike rate across first 500ms of light on, mean±SEM, n=34) as a function of step irradiance. Responses to stimulation of the dominant eye or both eyes together were statistically indistinguishable (F test; P=0.91). (G) Normalised acute response of binocular cells (conventions as in F, n=17). Binocular responses were significantly greater than those driven by the dominant eye alone (F test; P=0.004).

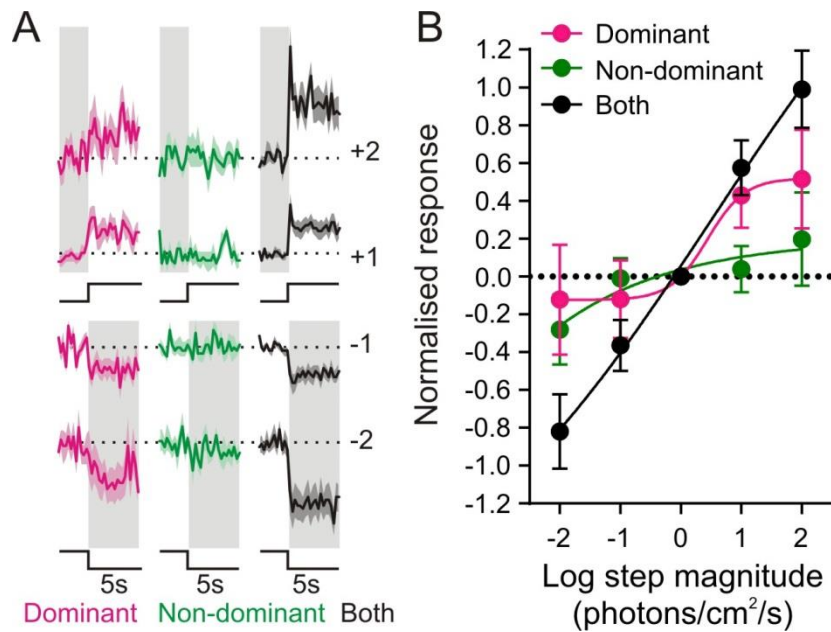


**Figure 4. Binocular integration is required for robust contrast responses in a subset of SCN neurons. (A)** Mean  $\pm$  SEM normalised response of binocular cells (n=17) to irradiance steps (-2 to +2 log units; 405nm LED) applied to one or both eyes under light adapted conditions (11.4 to 14.4 log photons/cm<sup>2</sup>/s). **(B)** Quantification of data in **A** showing change in firing over first 500ms of light step. Contrast responses were significantly larger upon stimulation of both eyes vs. the dominant eye only (F test, P=0.02).

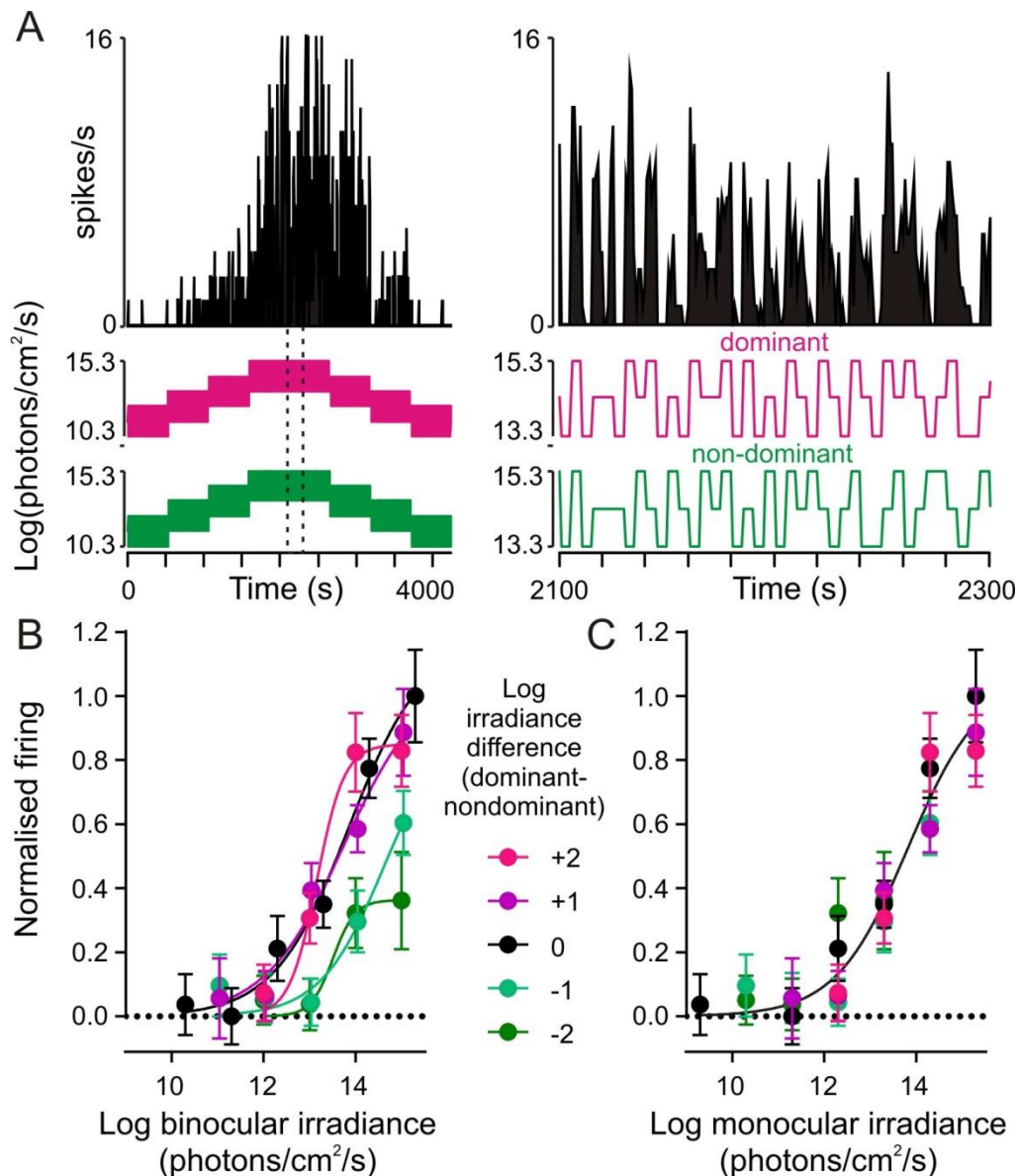


**Figure 5. SCN binocular cells encode monocular irradiance.** **(A)** Firing activity of a binocular SCN neuron presented with a pseudorandom irradiance sequence (see methods). Right panels show a portion of the responses at higher temporal resolution (indicated by the dotted region bottom left). **(B)** Normalised steady state firing activity of binocular cells (spikes occurring 4-5s after a step in irradiance; mean $\pm$ SEM, n=17) plotted as a function of the average irradiance across the two eyes and split according to the interocular difference in irradiance. When expressed in this manner, irradiance response relationships could not be described by a single sigmoid curve (F-test,  $P < 0.001$ ). **(C)** Data from **B** plotted according to irradiance at the dominant eye. Under these conditions, all data could be described by a single curve (F test,  $P = 0.62$ ).



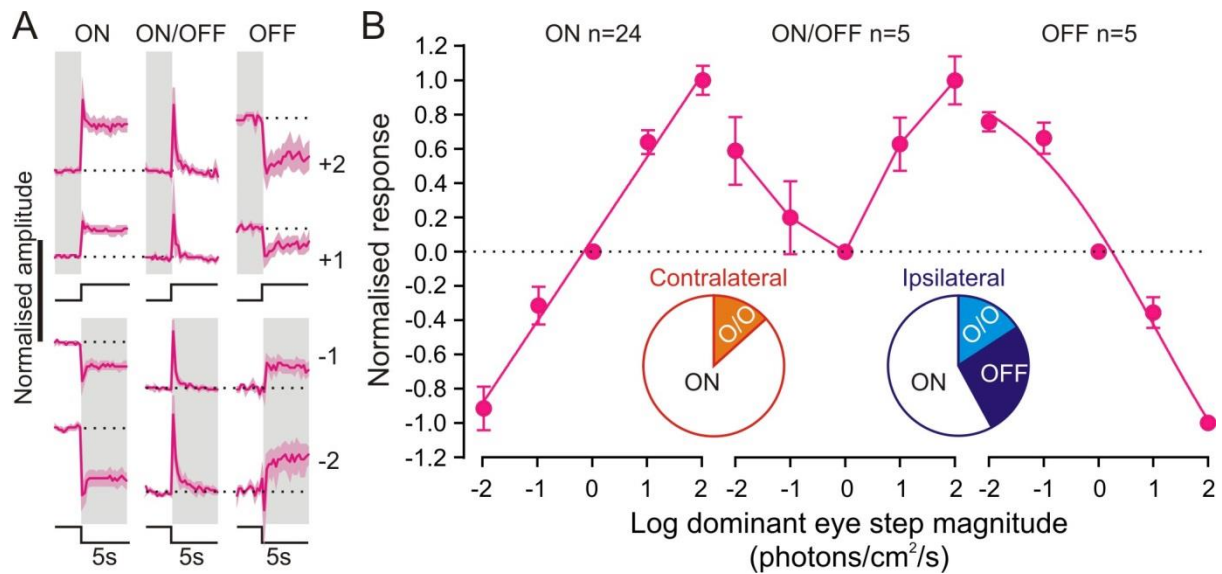


**Figure 6. Monocular SCN neurons exhibit varying responses to visual contrast. (A)** Mean $\pm$ SEM normalised response of monocular cell subpopulations to irradiance steps (-2 to +2 log units; 410nm LED) applied to the dominant eye under light adapted conditions (11.4 to 14.4 log photons/cm<sup>2</sup>/s). For most cells changes in firing rate were positively related to step magnitude (ON, n=24), while other cells showed the inverse relationship (OFF, n=5) or increased firing in response to both increase and decreases in irradiance (ON/OFF, n=5). **(B)** Quantification of data in **A** showing change in firing over first 500ms of light step for the three populations. Inset pie charts indicate the proportion of each cell type driven by either eye (n=15 and 19 total for contralateral and ipsilateral respectively). Note, OFF cells were all driven by the ipsilateral eye.

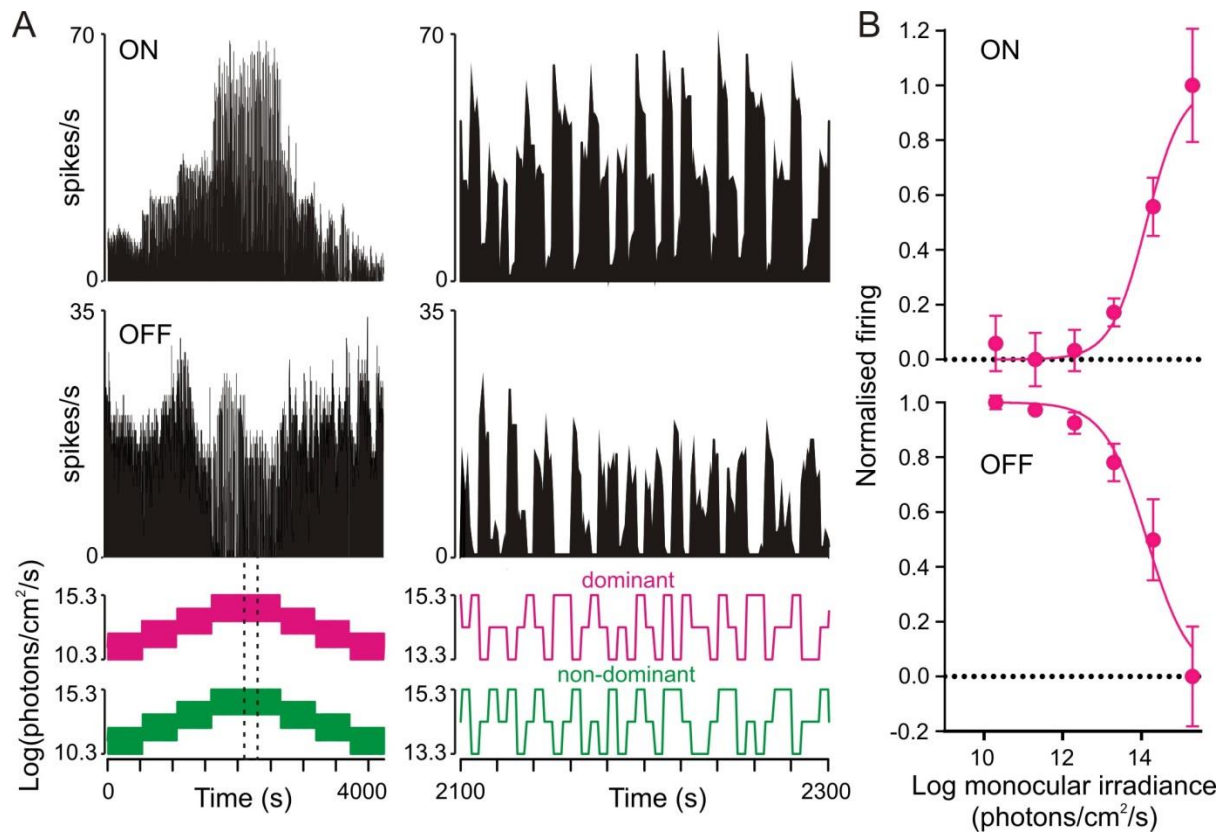


**Figure 7. Brightness and darkness coding in SCN monocular cells.** (A) Firing activity of simultaneously recorded ON (top) and OFF (bottom) SCN neurons presented with a pseudorandom irradiance sequence (see methods). Right panels show a portion of the responses at higher temporal resolution (indicated by the dotted region bottom left). (B) Normalised steady state firing activity of monocular ON and OFF cells (spikes occurring 4-5s after a step in irradiance; mean $\pm$ SEM, n=24 & 5 respectively) plotted as a function of irradiance at the dominant eye.

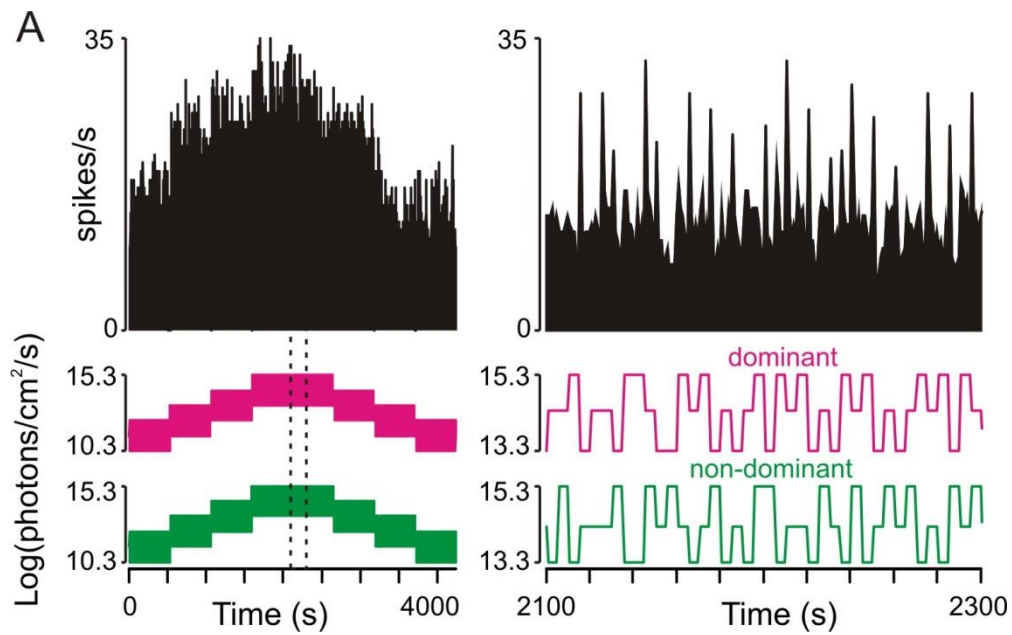


**Figure 8. SCN ON/OFF cells do not track irradiance. (A)** Firing activity of an ON/OFF SCN neuron presented with a pseudorandom irradiance sequence (see methods). Right panels show a portion of the responses at higher temporal resolution (indicated by the dotted region bottom left). Note that steady state firing does not vary as a function of irradiance.

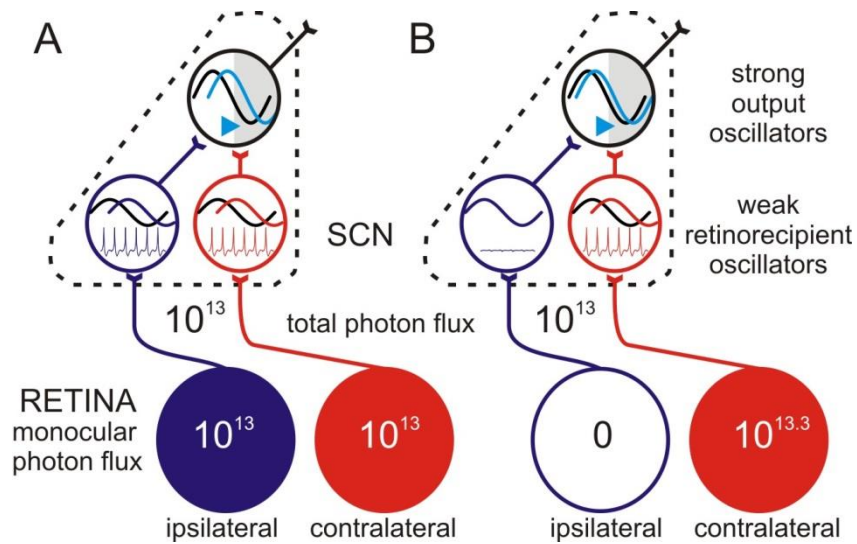


**Figure 9. Model of binocular integration in the SCN.** Retinorecipient clock cells, with easily perturbed oscillators are reset according to ‘local’ irradiance (at most brightness across one visual hemisphere). Strong output oscillators integrate circadian signals from the retinorecipient cells and adjust their phase according to the average of this input. As a consequence, illumination of both eyes drives a substantially larger adjustment in clock output (**A**) than a 2-fold increase in irradiance applied to just one (**B**).